

Demonstration of a thick holographic Stokesmeter

Jong-Kwon Lee *, John T. Shen, Alexander Heifetz, Renu Tripathi, M.S. Shahriar

*Center for Photonic Communications and Computing, Department of Electrical and Computer Engineering, Northwestern University,
2145 N Sheridan Road, Evanston, IL 60208, United States*

Received 13 July 2005; received in revised form 19 September 2005; accepted 23 September 2005

Abstract

A holographic Stokesmeter has the potential to be useful in high-speed polarization imaging applications. Highly polarization-sensitive gratings are an important component for this device. Using two sets of multiplexed gratings, we measured the Stokes parameters for three different polarization states of an input beam. These measured values compared well to values measured using the quarter-wave plate/linear polarizer method. This establishes the feasibility of such a Stokesmeter in its original configuration. We demonstrate further the basic mechanism behind a compact architecture for this device, requiring only a single substrate and a single imaging system, and describe a spectrally scanned polarimetric imaging system.

© 2005 Elsevier B.V. All rights reserved.

Keywords: Holography; Volume holographic gratings; Stokes parameter

Polarization imaging [1–3] can discriminate a target from its background in situations where conventional imaging methods fail. Identifying the components of the polarization of light reflected from a target allows one to construct an image that corresponds to the target's unique polarimetric signature. This is useful in applications ranging from target recognition to vegetation mapping [4–6]. Identifying the Stokes vector of the scattered light completely characterizes the polarization of light [7]. Current polarization imaging systems include mechanical quarter-wave plate/linear polarizer combinations, photodetectors with polarization filtering gratings etched onto the pixels, and liquid-crystal variable retarders [8–10]. The mechanical system is limited by the fact that it must rotate the angle between the wave-plate and polarizer before determining each Stokes parameter. The etched photodetector systems cannot resolve the complete Stokes vector at this time. The liquid-crystal variable retarder system is similar to the mechanical sensor but with a liquid-crystal display replacing the wave plates and polarizers. This method is

still sequential and the time required to reset the display limits the device operation to ~ 10 Hz. Systems based on the wave plate/polarizer architecture that split the beam into four parts and calculate the parameters in parallel require a large number of optical components [11]. Grating based polarimeter uses multiply diffracted and dispersed orders, and can measure all four Stokes parameters in parallel, but always needs the order blocking filters to prevent overlapping between the multiple diffraction orders of the beam [12]. Use of these filters leads to unwanted scattering, and may not be suitable for polarimetric imaging.

A holographic Stokesmeter (HSM) can be used to resolve all four Stokes components in parallel and at a high speed [13]. For a typical thick holographic grating, the response time of the device can be on the order of 10 ps. This removes the device as the bottleneck in the imaging system and instead the desired signal-to-noise ratio and detector parameters set the upper limit on the speed of the imaging process. The HSM [13] consists of two substrates each containing two volume gratings and a quarter-wave plate. The incoming beam is split and one half diffracts from the first set of multiplexed gratings, while the second half passes through the quarter-wave plate before diffracting from

* Corresponding author. Tel.: +8474913055.
E-mail address: jklee-7@northwestern.edu (J.-K. Lee).

the second set of multiplexed gratings. Measurements of the four diffracted intensities are used in a set of pre-weighted equations to determine the four Stokes parameters. This architecture can be analyzed using a set of Mueller matrices for each grating which then yields the measurement matrix of the system. The measurement matrix relates the observed signals to the incident Stokes vector as follows [13]:

$$\begin{bmatrix} I_{t1} \\ I_{t2} \\ I_{t3} \\ I_{t4} \end{bmatrix} = \begin{bmatrix} A_1 + B_1 & (A_1 - B_1) \cos(2\gamma_1) & (A_1 - B_1) \sin(2\gamma_1) & 0 \\ A_2 + B_2 & (A_2 - B_2) \cos(2\gamma_2) & (A_2 - B_2) \sin(2\gamma_2) & 0 \\ A_3 + B_3 & (A_3 - B_3) \cos(2\gamma_1) & 0 & -(A_3 - B_3) \sin(2\gamma_1) \\ A_4 + B_4 & (A_4 - B_4) \cos(2\gamma_2) & 0 & -(A_4 - B_4) \sin(2\gamma_2) \end{bmatrix} \begin{bmatrix} I \\ Q \\ U \\ V \end{bmatrix}. \quad (1)$$

Here, (I, Q, U, V) represents the input Stokes parameters, and I_{ti} is the diffracted intensity from the i th grating. $A_i (B_i)$ characterizes the diffraction efficiencies of the i th grating for s (p) – polarized input beams, taking into account the Fresnel reflections and transmissions at the interfaces. The angle $\gamma_1(\gamma_2)$ denotes the rotation of the substrate containing grating 1 and 3 (2 and 4). In order for the system to be well conditioned [14,15], the diffraction efficiencies of the four gratings need to be chosen properly along with the other parameters. Previously, we have reported on the polarization dependence of the diffraction of holographic gratings [16,17], and in this paper, we demonstrate the complete operation of the HSM.

The HSM was made from a 2 mm thick Memplex [18] sample with a 532 nm frequency doubled Nd:YAG laser. We employed two sets of multiplexed gratings using rotation angles of $\gamma_1 = -4^\circ$ and $\gamma_2 = 4^\circ$. Each set was written at external angles of 40° and 54° for the first and second gratings, respectively, with the reference beam at a 2° angle.

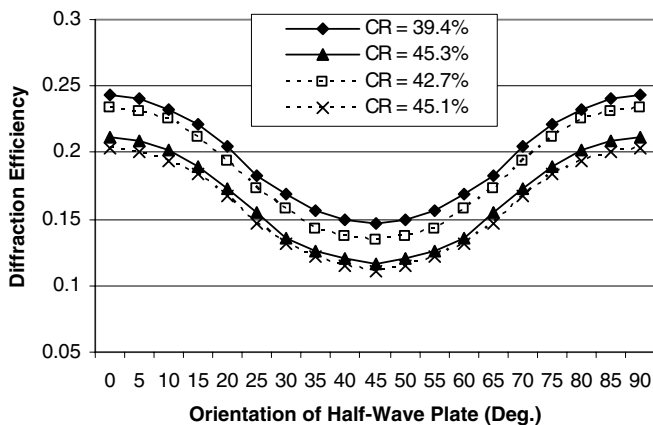


Fig. 1. Diffraction efficiencies vs. incident polarization of the two multiplexed HSM gratings, shown for four different contrast ratios (CR).

Fig. 1 displays the diffraction efficiencies of the holographic samples. It shows the polarization-sensitive diffraction efficiencies of 0.2429, 0.2114, 0.2343, and 0.2029 for the s-polarized state, and 0.1471, 0.1157, 0.1343, and 0.1114 for the p-polarized state. These diffraction efficiencies yield contrast ratios (CR) of 39.4%, 45.3%, 42.7%, and 45.1%, respectively. Here, CR is defined as the ratio of the difference between the diffraction efficiency of an s-polarized

wave and that of a p-polarized wave to the diffraction efficiency of an s-polarized wave. Using the above parameters we constructed the measurement matrix for our system.

The experimental readout setup for the HSM is illustrated in Fig. 2(a). We considered three different polarizations of the input beam: horizontal linear $[1, 1, 0, 0]$, linear $[1, -0.55, 0.84, 0]$, and elliptical $[1, 0.9, -0.25, -0.36]$. These polarization states can be realized by passing the laser beam through a half-wave and a quarter-wave plate rotated by appropriate angles. The intensity of each of the four diffracted beams was measured and used in the measurement matrix to determine the original Stokes vector.

For comparison, the values of the Stokes parameters describing the input polarization states were measured with a quarter-wave plate and a linear polarizer. This setup is illustrated in Fig. 2(b). In this conventional method, we need to measure the four different intensities $I(0,0)$, $I(45,0)$, $I(45,90)$ and $I(90,0)$ by changing the angle of the linear polarizer, and inserting the quarter-wave plate. Here, θ of $I(\theta, \Phi)$ is the angle of the linear polarizer, and Φ of $I(\theta, \Phi)$ is the quarter-wave plate retardation. The output intensity for this method is given as [19]:

$$I_{out}(\theta, \Phi) = (1/2)[I + Q \cos(2\theta) + U \cos(\Phi) \sin(2\theta) + V \sin(\Phi) \sin(2\theta)]. \quad (2)$$

From these intensity measurements we can calculate the Stokes parameters:

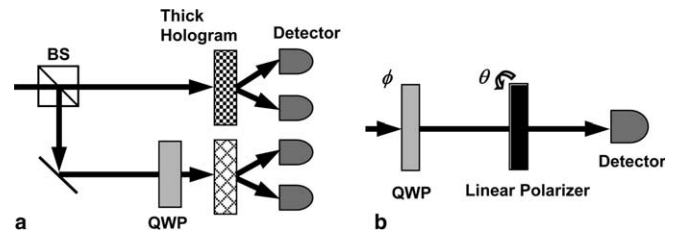


Fig. 2. Readout setup for (a) HSM, (b) conventional method using QWP/linear polarizer (QWP: quarter-wave plate; BS: beam splitter).

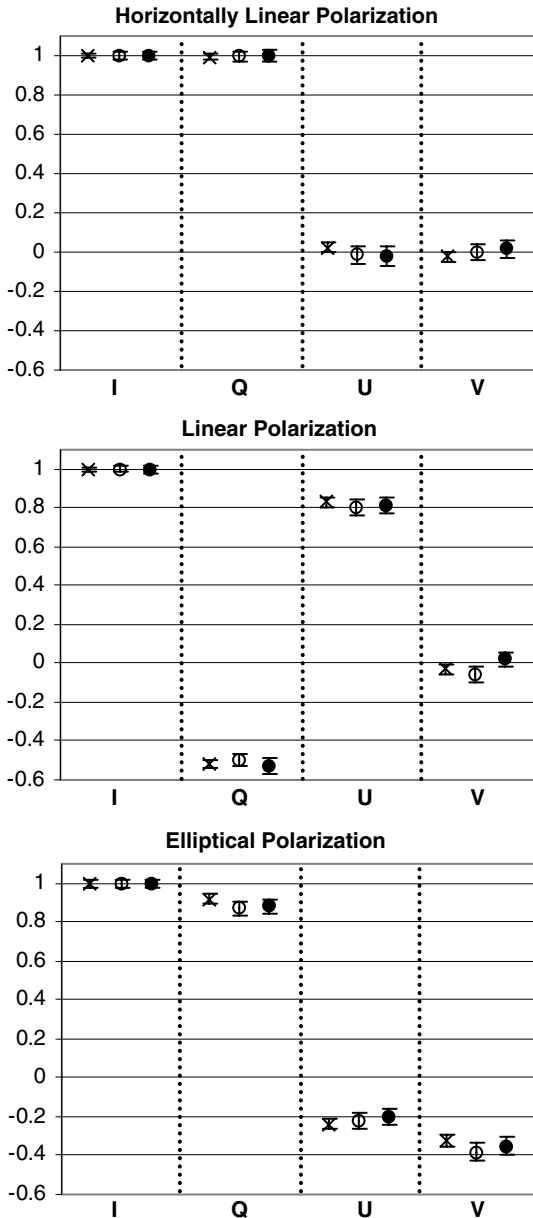


Fig. 3. The average values and the standard deviations of I , Q , U and V measured by the three methods for the three different polarization states of the input beam, where x -axis represents the Stokes parameters, and y -axis shows the normalized values thereof (Quarter-wave plate and linear polarizer: \times ; HSM: \circ ; New HSM: \bullet).

$$\begin{aligned}
 I &= I(0, 0) + I(90, 0), \\
 Q &= I(0, 0) - I(90, 0), \\
 U &= 2I(45, 0) - I(0, 0) - I(90, 0), \\
 V &= (2I(45, 90) - I(0, 0) - I(90, 0))/\eta,
 \end{aligned}
 \tag{3}$$

where η is the absorption factor related to the quarter-wave plate.

Fig. 3 displays the measured average values and the standard deviations of I , Q , U and V for each method (the conventional method “ \times ” and the HSM method “ \circ ”). Although the result for the HSM has a slightly larger error than the result for the quarter-wave plate/linear polarizer,

the average values are approximately equal to the assumed values within the error range. Note that the error in our conventional method is as high as 8%. This implies that the reference optical elements (such as the polarizer, waveplates, etc.) contribute significantly to the error observed in the HSM data. More precise optical elements can be used to suppress these errors. In general, residual error in the HSM drops monotonically with increasing CR, which can be seen from an analysis of the robustness of this HSM [16]. The current gratings used in this HSM had CRs in the range of 40–50%. We expect that a HSM made with much higher CR’s will be more accurate.

The architecture described above needs two holographic substrates with four different imaging systems to construct a polarimetric image. In order to use a single imaging system, we now describe an improved version of the HSM, and report a successful demonstration of the basic principle underlying it. This architecture consists of a pair of spatially separated gratings in a single holographic substrate and two electro-optic modulators (EOM), as shown in Fig. 4(a). The first EOM plays the role of the quarter-wave plate in the older architecture, namely to interchange the U and V parameters. In the new architecture, it is necessary to have the ability to reverse the polarization states of the input beams (s-polarization into p-polarization and p-polarization into s-polarization). This can be accomplished by rotating the fast axis of the second EOM by 45° with respect to that of the first EOM, where the second EOM has the same role of the half-wave plate. Fig. 4(b) shows a possible sequence of driving voltages for the EOMs, which can be operated at very high (\sim GHz) frequencies. Since there is 0 V sent to the EOMs during T_1 , the split input beams enter the holographic optical element (HOE) without changing the polarization state. Then, the measured intensities from the diffracted beams yield the information about the first two rows of the measurement

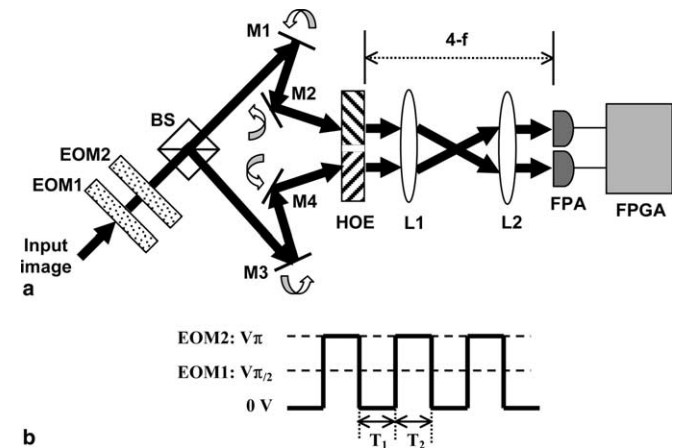


Fig. 4. (a) Polarimetric imaging system using two EOMs and a single holographic substrate, (b) input voltage signal scheme of two EOMs (EOM: electro-optic modulator; BS: beam splitter; HOE: holographic optical element; M: mirror; L: lens; FPA: focal plane array; FPGA: field programmable gate arrays).

matrix in Eq. (1). The intensity measurement for the reversed polarization states of the input beams after interchanging U and V parameters during T_2 yields the information about the third and fourth rows of the measurement matrix in Eq. (1). To implement the polarimetric imaging system using this new HSM, the output beams diffracted in parallel by the HOE are imaged onto two focal plane arrays (FPA) using a single $4f$ imaging system, as illustrated in Fig. 4(a). After all the four intensity measurements are taken during the periods of T_1 and T_2 for each pixel of the FPAs, we can construct the polarimetric image by manipulating the signals with precalibrated field programmable gate arrays (FPGA). We have implemented the basic model of this new HSM by using a quarter-wave plate and a half-wave plate in place of the two EOMs. The Stokes parameters measured this way are also added in Fig. 3 (new HSM'●'), and agree well with the previous methods, thus establishing the feasibility of this architecture.

This new HSM is structured to accommodate the ability to perform spectrally multiplexed polarimetry as well. Specifically, the single hologram in each zone of the substrate could be replaced by a set of angle multiplexed gratings. Each grating would be designed to produce a diffracted beam (orthogonal to the substrate) only for a specific band of frequencies at a specific angle of incidence. Thus, by scanning the angle of incidence without changing the position [20], it is possible to produce a polarimetric image for a desired wavelength band. For substrates with a thickness of 1 mm, for example, the spectral width of each band is of the order of 0.5 nm in the visible range, and the corresponding Bragg angular bandwidth is about 1 mrad. Thus, it may be possible to implement many such bands in a single device. The maximum number of bands would in practice be limited by the M/λ of the material [21].

In conclusion, we have performed measurements of arbitrary Stokes parameters with an HSM that consists of two substrates each containing two volume gratings. Measured Stokes parameters are compared with the ones obtained by a conventional method. The values measured for both methods are approximately equal to the assumed

ones within the measurement error range. This shows the feasibility of an HSM in its original configuration. We also demonstrate the basic mechanism behind a compact version for this device using only a single substrate and a single imaging system, and describe a spectrally scanned polarimetric imaging system. The ability to combine spectral discrimination with polarization imaging in a single device makes this HSM a unique device of significant interest.

References

- [1] J.L. Pezzaniti, R.A. Chipman, *Opt. Eng.* 34 (1995) 1558.
- [2] K.P. Bishop, H.D. McIntire, M.P. Fetrow, L. McMackin, *Proc. SPIE* 3699 (1999) 49.
- [3] G.P. Nordin, J.T. Meier, P.C. Deguzman, M.W. Jones, *J. Opt. Soc. Am. A* 16 (1999) 1168.
- [4] L.J. Denes, M. Gottlieb, B. Kaminsky, D. Huber, *Proc. SPIE* 3240 (1998) 8.
- [5] T. Nee, S.F. Nee, *Proc. SPIE* 2469 (1995) 231.
- [6] P.J. Curran, *Remote Sens. Environ.* 12 (1982) 491.
- [7] A. Gerrard, J.M. Burch, *Introduction to Matrix Methods for Optics*, Dover Publications, New York, 1974.
- [8] D.H. Goldstein, *Appl. Opt.* 31 (1992) 6676.
- [9] J.L. Pezzaniti, R.A. Chipman, *Proc. SPIE* 2297 (1994) 468.
- [10] J.M. Bueno, P. Artal, *Opt. Lett.* 24 (1999) 64.
- [11] V.L. Gamiz, *Proc. SPIE* 3121 (1997).
- [12] S. Krishnan, S. Hampton, J. Rix, B. Taylor, R.M.A. Azzam, *Appl. Opt.* 42 (2003) 1216.
- [13] M.S. Shahriar, J.T. Shen, R. Tripathi, M. Kleinschmitt, T. Nee, S.F. Nee, *Opt. Lett.* 29 (2004) 298.
- [14] A. Ambirajan, D.C. Look, *Opt. Eng.* 34 (1995) 1651.
- [15] D.S. Sabatke, A.M. Locke, M.R. Descour, W.C. Sweatt, J.P. Garcia, E.L. Dereniak, S.A. Kemme, G.S. Phillips, *Proc. SPIE* 4133 (2000) 75.
- [16] M.S. Shahriar, J.T. Shen, M.A. Hall, R. Tripathi, J.K. Lee, A. Heifetz, *Opt. Commun.* 245 (2005) 67.
- [17] T.W. Nee, S.F. Nee, M.W. Kleinschmitt, M.S. Shahriar, *J. Opt. Soc. Am.* 21 (2004) 532.
- [18] Burzynski, D.N. Kumar, S. Ghosal, D.R. Tyczka, *Holographic Recording Material*, US Patent No. 6,344,297 (2002)..
- [19] Dennis Goldstein, *Polarized Light*, second ed., Marcel Dekker, Inc., New York, 2003.
- [20] M.S. Shahriar, R. Tripathi, M. Kleinschmitt, J. Donghue, W. Weathers, M. Hug, J.T. Shen, *Opt. Lett.* 28 (2003) 7.
- [21] H.N. Yum, P.R. Hemmer, R. Tripathi, J.T. Shen, M.S. Shahriar, *Opt. Lett.* 29 (2004) 15.